NJC

Effects of Dynamic Vulcanization on Kinetics of Isothermal Crystallization in a Miscible Polymeric Blend

Journal:	*New Journal of Chemistry*
Manuscript ID:	NJ-ART-03-2015-000514.R1
Article Type:	Paper
Date Submitted by the Author:	07-May-2015
Complete List of Authors:	Abolhasani, Mohammad Mahdi; University of Kashan, Chemical Engineering

Effects of Dynamic Vulcanization on Kinetics of Isothermal Crystallization in a Miscible Polymeric Blend

Mohammad Mahdi Abolhasani*[a]

[a]Chemical Engineering Department, University of Kashan, Kashan, Iran

Abstract

In this study kinetics of isothermal crystallization was used as a tool to investigate effect of dynamic vulcanization on phase separation of miscible blends of acrylic rubber (ACM) and Poly(vinylidene fluoride) (PVDF). Morphological studies using Scanning electron microscopy (SEM) clearly showed that crosslinking upon dynamic vulcanization induced nano-scale ACM droplets in the samples near the phase separation curve. Real-time Fourier transform infrared spectroscopy (FTIR) and differential scanning calorimetry (DSC) were used to study skeletal change of the chains during the isothermal crystallization and kinetics of the crystallization, respectively. FTIR study demonstrated that PVDF crystallizes in α form in blends and in dynamically vulcanized samples. Avrami analysis showed that n values of dynamically vulcanized samples are larger than that of corresponding unvulcanized blends. Crystallization kinetics evaluated using Lauritzen-Hoffman theory proved that the increasing of the free energy of folding (σ_e) upon blending of ACM with PVDF while dynamic vulcanization reduced this parameter. free energy of folding studies confirms SEM results demonstrating phase separation upon dynamic vulcanization in this blend.

Keywords: Dynamic vulcanization, Crystallization kinetics, Free energy of folding, Phase separation

* To whom correspondence should be addressed. E-mail: abolhasani@kashanu.ac.ir

Introduction

Crystallization kinetics of crystalline/noncrystalline miscible blend has been studied extensively in the past 40 years. Generally, a reduction on the growth rate of crystallizable component upon addition of amorphous polymer is expected [1-7]. This phenomenon is related to increment of glass transition temperature (T_g) and the dilution of crystalline polymer at growth front [3, 8]. Nonetheless, less effort has been done to study the crystallization kinetics of a semi-crystalline polymer in a miscible blends containing one vulcanizable rubber [8-14]. In such blends, vulcanization results in crosslinking, branching and substantial changes in physical and chemical properties of amorphous rubbery phase, this can affect the free energy of nucleation and chains movement, and therefore might have significant effect on kinetic of crystallization. Investigation of kinetics of isothermal crystallization on a partially phase separated structure upon dynamic vulcanization is a very complex issue. The topological effects of 3D structure of vulcanized polymer on kinetics of crystallization and phase separation have to be considered. Therefore it is worthy to study the crystalline structure and kinetics of this kind of vulcanizable miscible blend.

Some researchers showed previously significant influence of curing on crystallization kinetics and miscibility of miscible thermoset blends [8, 10-13]. It is known that increase in molecular weight of each polymer in a miscible blend would reduce the entropy of mixing. Therefore, phase decomposition originate from crosslinking is likely for blends with a positive enthalpy of mixing [9, 11].

Kyu et al. [15] investigated influence of static vulcanization on phase separation of syndiotactic polypropylene(sPP)/ethylene propylene diene monomer (EPDM) blends. Opposing to previous studies [8, 10-13] they demonstrated that vulcanization induced phase decomposition in sPP/EPDM miscible blend. As stated above static curing of thermosetting miscible blends has been extensively studied in the literature but there is little effort on exploring the effects of dynamic vulcanization process, in which crosslinking reactions are take place during the mixing, on miscibility and crystallization kinetics of miscible systems.

Poly(vinylidene fluoride) (PVDF) as a polymorphous crystallizable polymer has at least five crystal polymorphs, i.e., α, β, γ, ε and δ [16-18]. There are many reports in the literature showed the effectiveness of nano-fillers on induction of β polymorph in PVDF film. However, to the best of our knowledge no one investigated effects of nano-scale phase separated structure on polymorphism of PVDF.

Recently we have investigated miscibility of PVDF/ACM(Acrylic rubber) blend and influence of dynamic vulcanization on processability and morphology of this system [2, 19, 20]. We demonstrated that PVDF and ACM are miscible in the blends with more than 50% ACM [2]. We also showed that crosslinking reaction induced nano-phase separated droplet in blends near the binodal curve whereas blends in miscible area were miscible even after dynamic vulcanization [20]. In this study we want to explore the complicated interrelationship between crosslinking of amorphous component and crystallization kinetics of crystallizable polymer. It is anticipated that dynamic vulcanization affects the kinetics of crystallization significantly. The key question of present paper is: does the crystallization kinetics study confirm that the dynamic vulcanization induced phase separation? In this work, effects of dynamic vulcanization on kinetics of crystallization of PVDF in PVDF/ACM miscible blends are presented (blends with more than 50% ACM).

Experimental

Materials and methods

PVDF (Kynar 710;Mw=70000, Mw/Mn=2) and acrylic rubber (Grade AR71;Mw=620000, Mw/Mn=9) were purchased from Arkema and Zeon Advanced Polymix Co., respectively. ACM is a copolymer of poly (ethyl acrylate) (PEA) and 5%w of chlorine cure-site monomer. Before processing polymers were dried in a vacuum oven at 80˚C for 12h. The blends without adding curative were prepared using a Brabender type plastic mixer with two rotors at a rotation speed of 100rpm at 190˚C for 10min. For dynamic vulcanization, sodium stearate(5phr) and magnesium oxide (10phr) as additives for curing process and 1phr sulfur as curing agent were added after mixing of PVDF and ACM for 10 min.

Vulcanized samples are denoted by the -C in the sample name in the text. Samples then were hot pressed into the films at 200˚C and allowed to slowly cool down to room temperature. Table 1. shows details of samples prepared for this study.

Table 1. Details of prepared samples

Sample	PVDF(wt%)	ACM(wt%)	Sulfur(phr)
PVDF	100	0	0
50/50	50	50	0
40/60	40	60	0
20/80	20	80	0
10/90	10	90	0
50/50-C	50	50	1
40/60-C	40	60	1
20/80-C	20	80	1
10/90-C	10	90	1

Characterization

Differential Scanning Calorimetery (DSC) was done with a TA Instrument Q200. Samples were melted at 210˚C for 10 min. Then each sample was cooled down to desired isothermal temperature and maintained at that temperature until the degree of crystallinity didn't increase any more. After completion of

isothermal crystallization the sample was subsequently reheated to 210˚C at a rate of 20˚C/min to obtain the melting endotherm curve. Degree of crystallinity was calculated according to:

$$X_t = \frac{\int_{t_0}^{t}(d_H/d_t)d_t}{\int_{t_0}^{\infty}(d_H/d_t)d_t} \quad (1)$$

where t_0 is the time at which the sample reaches isothermal conditions, indicated by a flat base line after an initial spike in the thermal curve.

FTIR spectra were collected at 2 cm^{-1} nominal resolution using a Bruker 70 spectrometer in transmission mode. The spectra were obtained by averaging 32 scans with a mean collection length of 1 s per spectrum. The background spectra at the same crystallization temperature (T_c) with the sample was collected and used for reduction. The homogenous mixtures of KBr powder and samples in the mass ratio 95:5 were prepared. The mixtures were then adapted into disks with a thickness of ~0.5 mm by pressing. The disks were placed in a homemade heating chamber, which allowed reaching the desired T_c at the rate of 50ºC/min like DSC technique. After attaining T_c, a time-resolved FTIR measurement was conducted.
The morphology and microstructure of samples was examined by scanning electron microscopy (SEM), Leica S440 equipment. Samples were cryogenically fractured in liquid nitrogen and then sputter-coated with a thin layer of gold prior to imaging.

Small-angle X-ray scattering (SAXS) experiments were conducted at the Australian Synchrotron on the small/wide angle X-ray scattering beam-line utilizing an undulator source that allowed measurement at a very high flux to moderate scattering angles (hs) and a good flux at the minimum scattering vector (q) limit (0.012 nm^{-1}). The intensity profiles were interpreted as the plot of scattering intensity (I) versus q:

$$q = (4/\lambda) \sin(\theta/2) \quad (2)$$

where λ is the wavelength and is equal to 0.062 nm. The scattering invariant, Q, was determined from the total integrated intensity, I(q) using [21]:

$$Q = \int I(q).q^2 dq \quad (3)$$

The one-dimensional electron density correlation function was obtained from [22]:

$$\gamma(x) = \frac{\int I(q).q^2 \cos(qx) dq}{Q} \quad (4)$$

where x is a dimension along the normal to the lamellar stacks. Parameters such as the long period, L, average crystalline thickness, l_c and amorphous layer thickness, l_a, were determined using the method of Strobl and Schneider [22].

Results and Discussion

Morphology of dynamically vulcanized PVDF/ACM blends

Effects of dynamic vulcanization on morphology of miscible blends of 20/80 and 50/50 are presented in Fig.1. Before dynamic vulcanization there is no sign of inhomogeneity in miscible blends of 20/80 and 50/50, while after dynamic vulcanization morphology of these two blends is completely different. Both of these blends after dynamic vulcanization (20/80-C and 50/50-C) revealed a powder liked coarse and porous structure, but in nanometer scale their morphology was different. Comparing Fig. 1.b with Fig. 1.d it is clear that 50/50-C blend is occupied by phase decomposed nano scale (<100nm) droplets while there is no sign of inhomogeneity in 20/80-C blend. As we stated previously[2, 20] since 50/50 blend is close the binodal curve, it can be concluded that crosslinking reaction upon dynamic vulcanization caused phase decomposition. Therefore at compositions close to the binodal curve nucleation is the phase decomposition mechanism thus dynamic vulcanization at metastable regions induced nano-phase separated structure for 50/50-C sample.

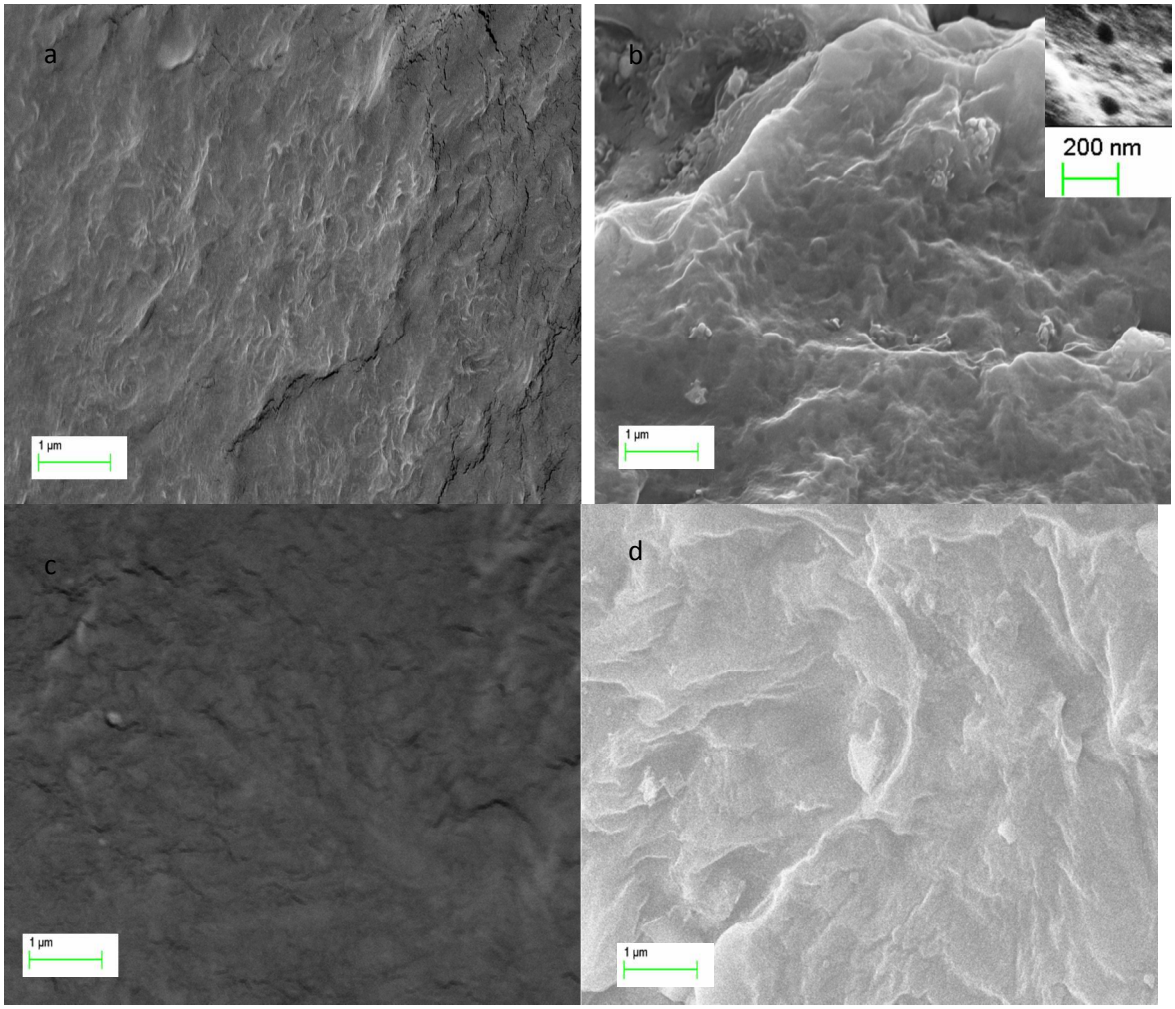

Figure 1. SEM micrographs of a) 50/50, b) 50/50-C, c) 20/80, d) 20-80-C, in inset of 50/50-C sample nano droplets induced by dynamic vulcanization are clearly observable.

SAXS analysis

SAXS method is a powerful technique to evaluate effects of dynamic vulcanization on lamellar structure of the samples. Lorentz-corrected SAXS profile of the 20/80 and 50/50 blends before and after dynamic vulcanization and their related linear correlation functions [22] are presented in Fig.2. By plotting simple geometric analysis of $\gamma(x)$ and assuming the corresponding two-phase model the values of the most probable long period (L), lamellar thickness (l_c) and amorphous layer thickness (l_a) can readily be evaluated. Fig.3 shows evaluation of above mentioned parameter for 20/80 and 50/50 blends. It is clear that for most of the blends the l_a and L decreased with dynamic vulcanization and this decrease is more pronounced for 50/50 blend compare to other samples. However, l_c, is almost unaffected by dynamic

vulcanization. It can be concluded that crosslinking reaction induced phase decomposition; therefore, l_a and L decreased as a result of ejection of ACM chains from amorphous layer of PVDF. Nevertheless, this phenomenon is much pronounced for 50/50 blend because as mentioned above this blend is close to the binodal curve. Therefore, lower driving force for phase separation is required to eject the ACM chains from the inter-lamellar space. Guo et al. [23] showed that Curing reaction can induce phase separation in an initially miscible Epoxy resin/thermoplastic blend using SAXS technique.

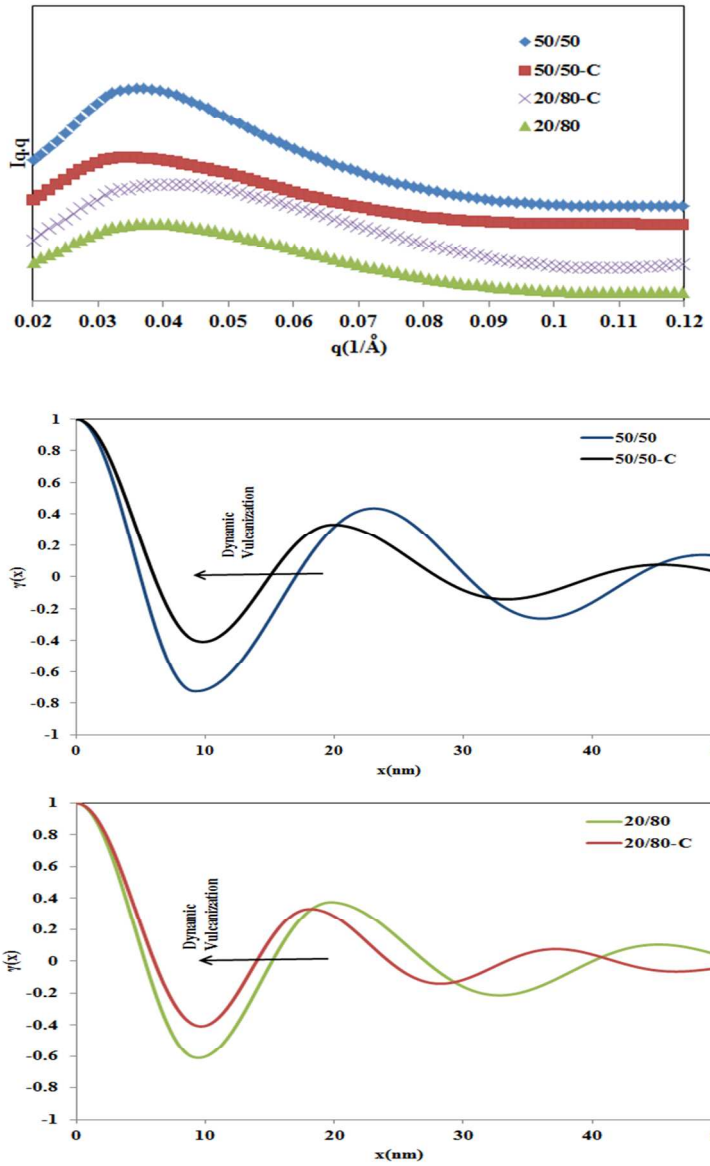

Figure 2. a) Lorentz corrected SAXS patterns of 50/50 and 20/80, and b) linear correlation functions for of 50/50 sample c) linear correlation functions for of 20/80 sample; before and after dynamic vulcanization.

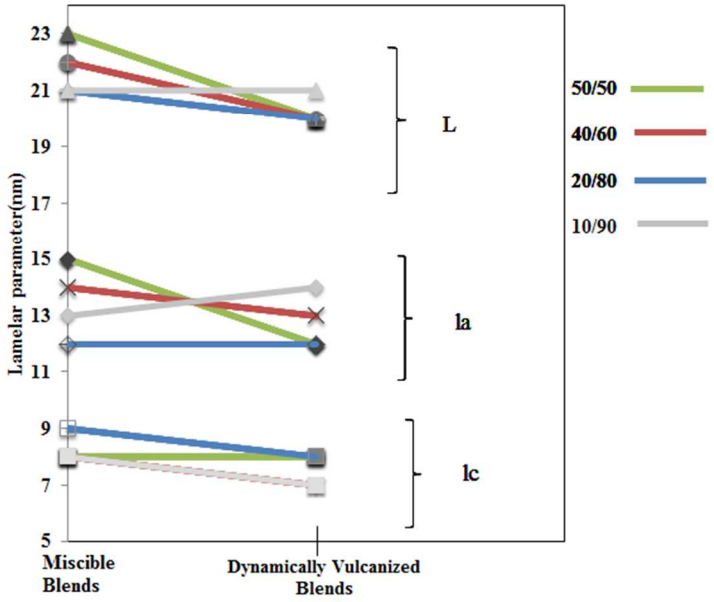

Figure3. Variations of lamellar for miscible blends and dynamically vulcanized blends

Effects of dynamic vulcanization and isothermal crystallization on polymorph formation of PVDF

Real-time FTIR were conducted at various isothermal crystallization temperatures T_c for neat PVDF, PVDF/ACM blends and dynamically vulcanized samples. Fig. 4 shows variation of FTIR spectra by time for neat PVDF during isothermal crystallization at 150ºC and 20/80 blend and dynamically vulcanized 20/80 blend at 120ºC in region of 1000–550 cm^{-1}. These spectrum shows only α characteristic peaks (975,795,763, 615cm^{-1}) of PVDF[20, 24-30] therefore blending and dynamic vulcanization does not induce creation of polymorphic crystalline forms of PVDF. It seems that unlike nanofillers nano-scale phase separated structure cannot induce electroactive polymorphs in PVDF.

Fig.5. shows the typical difference spectrum obtainable by subtracting the first spectra at melting condition from the successive spectrum of neat PVDF, 20/80 and 20/80-C samples related to Fig.4. The

bands with the negative sign are related to amorphous phase whereas the positive regions are related to crystalline phase peaks [31] . For all samples, the characteristic peaks of the α crystal form ascend and their intensities increase till the end of crystallization.

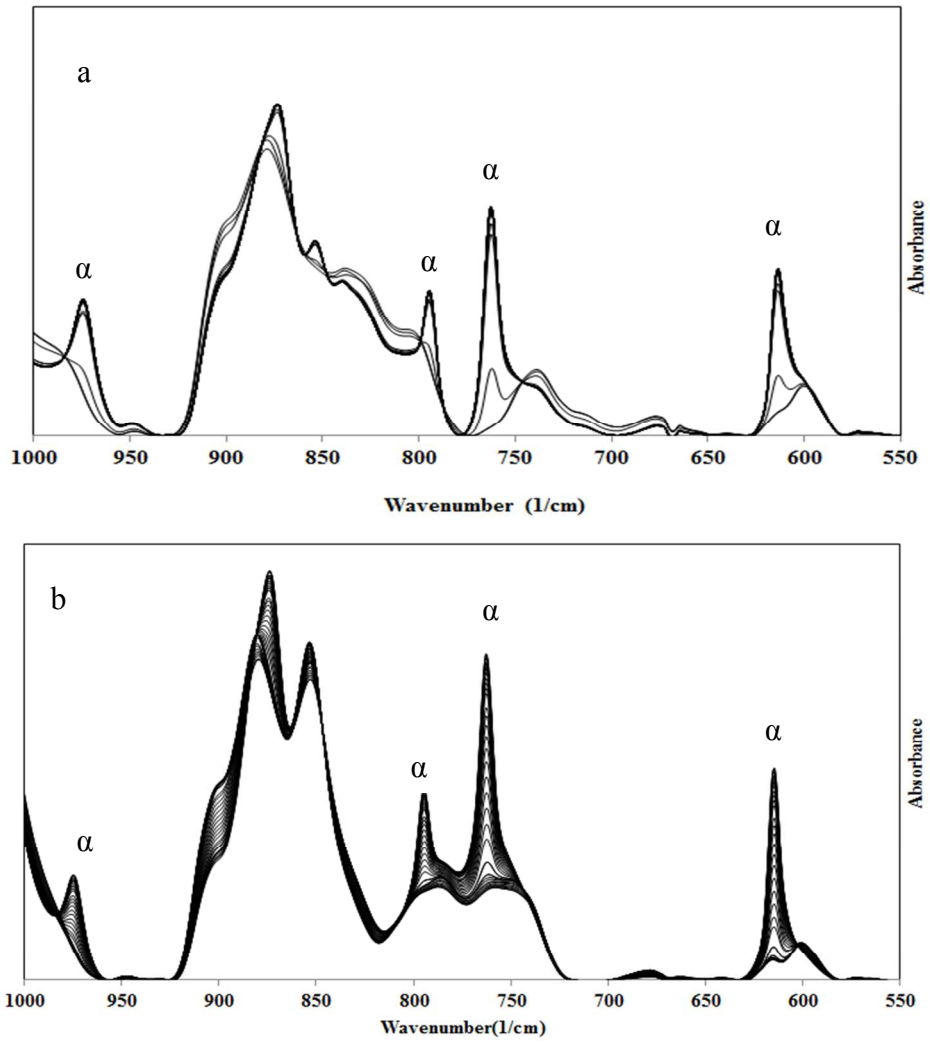

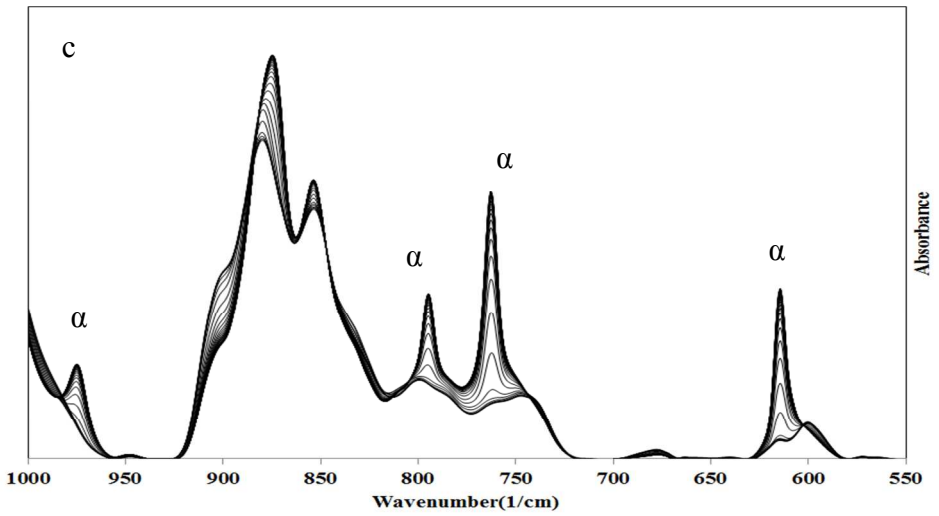

Figure4. Time-resolved spectra of a) neat PVDF at 150°C b) 20/80 and C) 20/80-C samples at 120°C

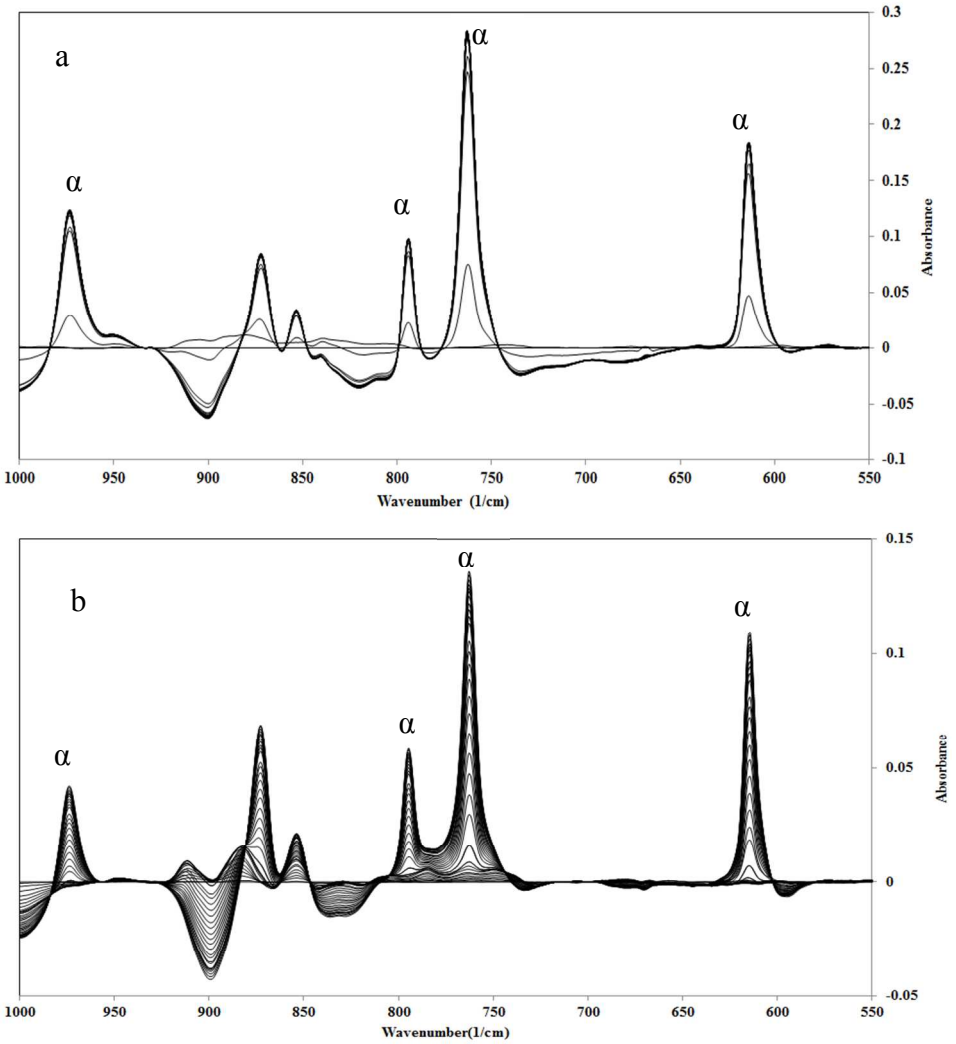

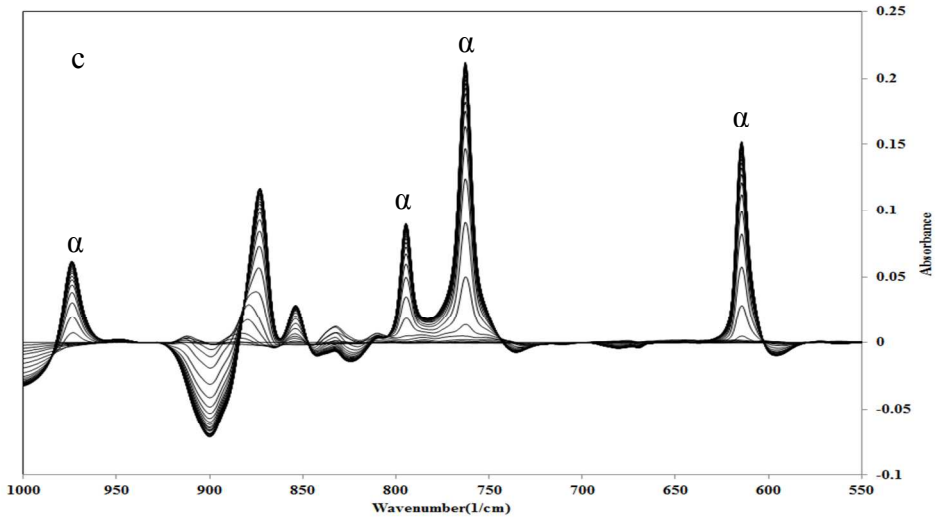

Figure5. Difference spectra of a) neat PVDF at 150°C b) 20/80 and C) 20/80-C blend at 120°C.

Rate of overall crystallization

Fig. 6 displays the evolution of the relative crystallinity X_t for neat PVDF, PVDF/ACM blends and dynamically vulcanized samples obtained by real-time FTIR (763cm^{-1} band was used as crystalline characteristic band) and DSC measurements. It is clear from Fig. 6 that slope of isotherms declines with increase of T_C, suggesting crystallization take place at right hand side of crystallization bell shape curve. Thus, nucleation is the controlling parameter in evaluation of the rate of overall crystallization of neat PVDF, PVDF/ACM blends and vulcanized samples. The half time of crystallization ($t_{1/2}$) evaluated using Fig.6 isotherms are presented in Fig. 7. As it is expected $t_{1/2}$ values obtained by DSC and real-time FTIR coincide which confirms the accuracy of performed experiments. From Fig.7 one can understand that (i) incorporation of noncrystallizable vulcanized and unvulcanized ACM component depressed the rate of overall crystallization of PVDF, (ii) increasing the percent of both vulcanized and unvulcanized ACM component decreased rate of overall crystallization considerably (iii) for most of the samples dynamic vulcanization decreased the overall crystallization rate compared to unvulcanized one.

The low chain mobility of the crosslinked ACM in the PVDF/ACM blends caused the vulcanized ACM molecules diffuse away slowly from the crystallization growth front, as compared to usual diluent

polymers in blends with PVDF. Therefore, the topology of network of crosslinked ACM has a significant effect on the crystallization of PVDF.

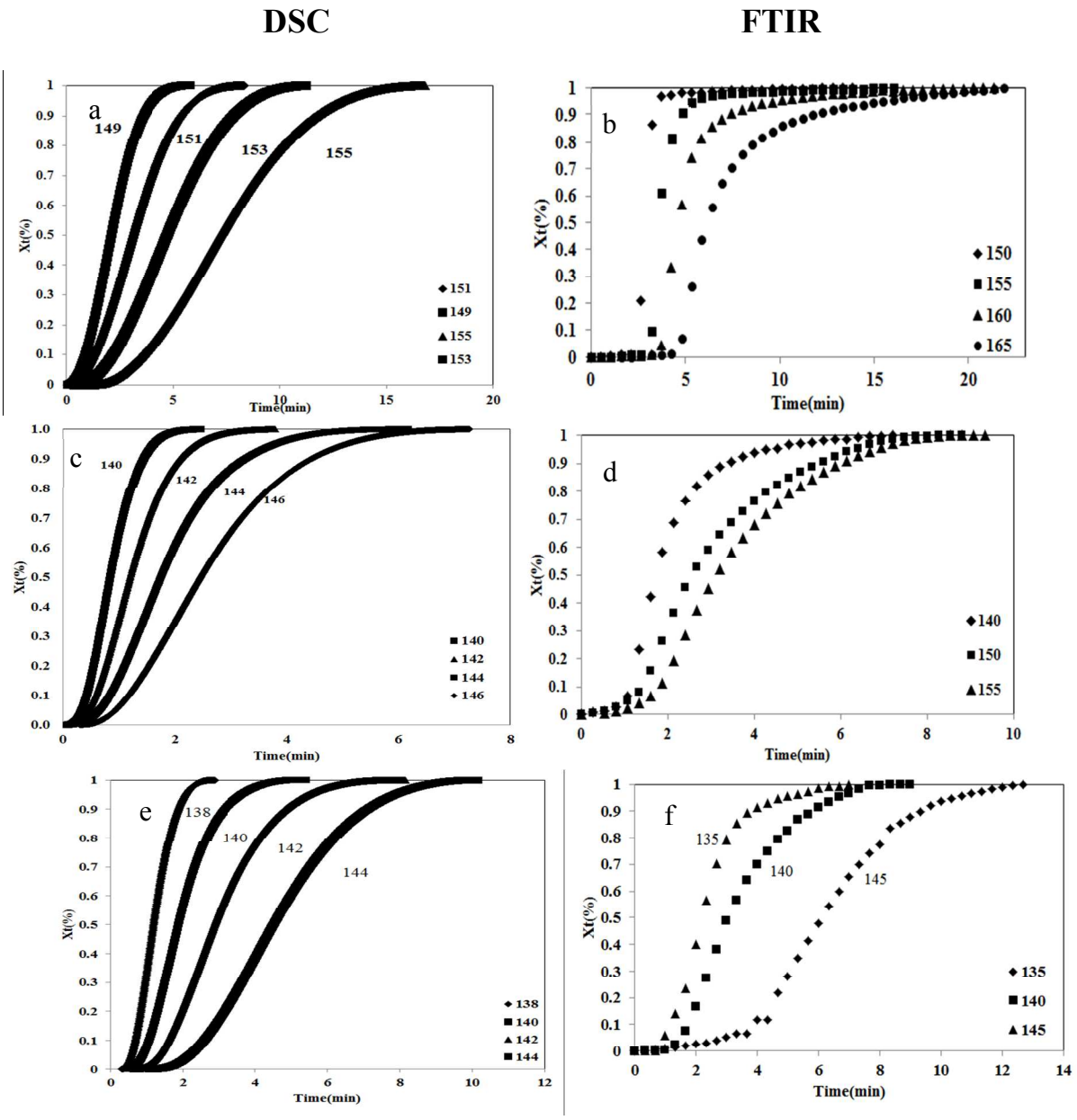

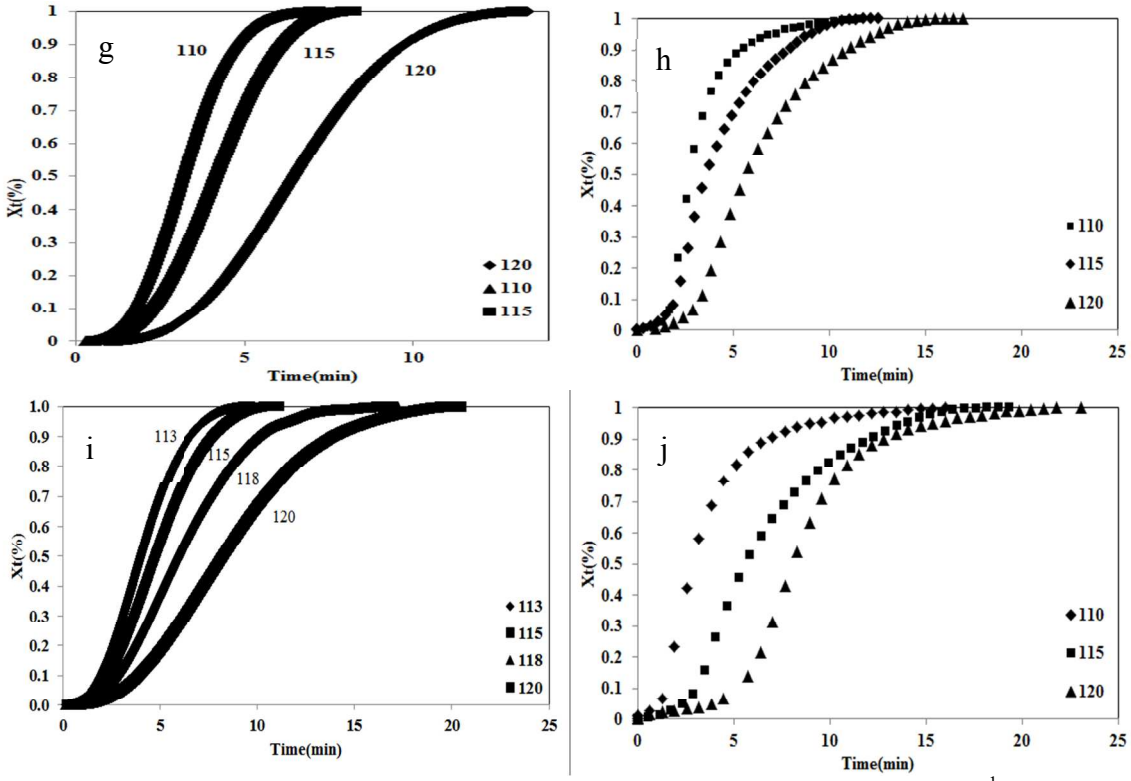

Figure6. X_t obtained by DSC and FTIR (time variation of reduced intensities for 763cm^{-1} band) a, b) neat PVDF, c, d)50/50, e,f)50/50-C, g,h)20/80, i,j)20/80-C blend.

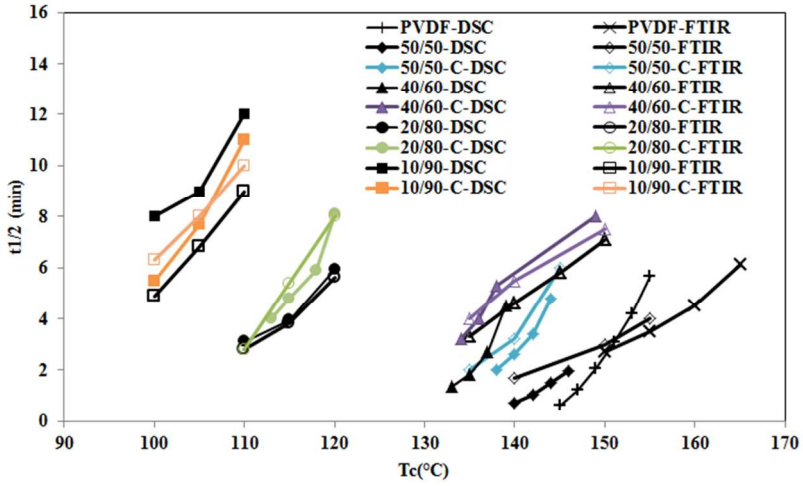

Figure7. half-time of crystallization($t_{1/2}$) for neat PVDF, unvulcanized and dynamically vulcanized blends obtained by DSC and real-time FTIR

Kinetics of isothermal crystallization

Avrami equation has been widely used in the literature to study the kinetics of the isothermal crystallization [32]

$$\log[-\ln(1-X_t)] = \log k_n + n \log t \quad (5)$$

Where K_n is the overall kinetic rate constant and n the Avrami index which depends on the nucleation and growth mechanism of the crystals.

Fig.8 presents the typical plots of $\log[-\ln(1-X_t)]$ vs. $\log t$ obtained by DSC experimental data for 20/80 and 50/50 unvulcanized and dynamically vulcanized blends. Only DSC analysis was used to study crystallization kinetics of this system. It is known that Avrami equation is only valid for early stage of crystallization [33], [34].

The experimental data at low conversion were used to calculate K_n and n. Table 2 lists the values of n and K_n calculated using the slopes and intercepts of Avrami curves.

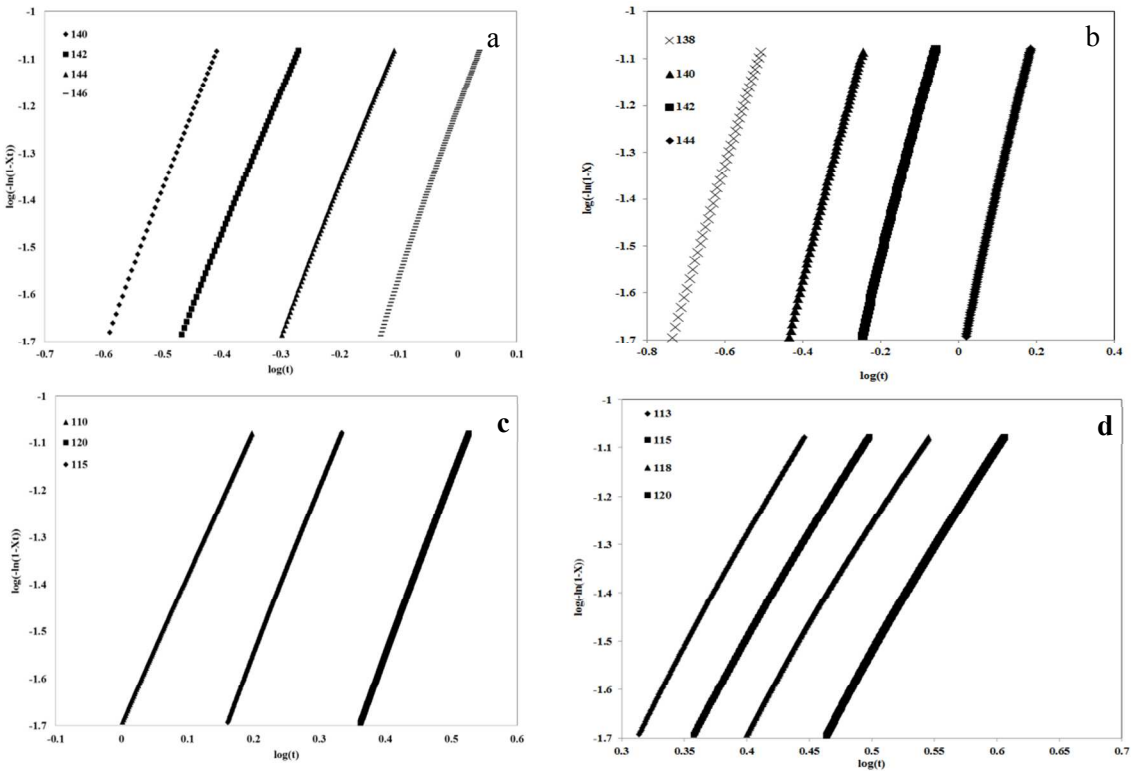

Figure8. plots of log(-ln(1-X_t)) vs. Log(t) for isothermal crystallization of a)50/50,b)50/50-C, C)20/80, d)20/80-C blends.

Opposing to theoretical prediction in all samples the values of n were non-integer; this observation is generally accounted for by mixed growth and/or surface nucleation and two-stage crystallization[8]. Grenier and Prud'hamme[35] stated that error in determination of the melting enthalpy and estimation of the 'zero' time is the cause of the non-integer values of n.

In Table 2, it can be seen that the values of n for dynamically vulcanized samples are higher than that of related unvulcanized samples. The n values of vulcanized blends are between 4 and 5 which can be related to the branching mechanism of macromolecular crystals. Morgan [36] showed that branching crystals have a higher values of n. From the above discussion it is obvious that increase in n values of vulcanized samples can be related to the branching mechanism of polymer crystals imposed to the system upon topological constraint of 3D network of crosslinked chains. Therefore, crystallization mechanism of PVDF in PVDF/ACM blends changes significantly after dynamic vulcanization of ACM. However, 50/50 vulcanized blend n values were lower than corresponding 50/50 unvulcanized blend.

Table 2. Avrami parameter for PVDF and blends.

Unvulcanized	Tc(˚C)	n	K(min^{-n})	Vulcanized	Tc(˚C)	n	K(min^{-n})
PVDF	149	2.3	1.35E-01				
	151	2.4	5.37E-02				
	153	2.9	1.12E-02				
	155	3.7	1.00E-03				
50/50	140	3.2	1.83E+00	50/50-C	140	2.66	1.86E+00
	142	3.0	5.53E-01		142	3.19	5.11E-01
	144	3.2	1.85E-01		144	3.23	1.36E-01
	146	3.6	6.27E-02		146	3.67	1.03E-02
40/60	133	3.0	2.52E-01	40/60-C	134	4.27	7.26E-02
	135	3.0	1.09E-01		136	4.78	1.00E-02
	137	3.0	3.48E-02		138	4.56	3.12E-03
	139	3.0	7.33E-03		148	4.33	1.14E-03
20/80	110	3.1	2.04E-02	20/80-C	113	4.61	7.56E-04
	115	3.5	5.57E-03		115	4.36	5.73E-04
	120	3.7	9.12E-04		118	4.18	1.51E-04
					120	4.29	9.80E-05
10/90	100	2.7	2.04E-03	10/90-C	100	4.01	4.55E-03
	105	3.0	5.57E-03		105	4.66	4.75E-04
	110	3.1	9.12E-04		110	3.58	4.87E-04

Equilibrium melting points

Using melting point temperature ($T_m^{'}$) against crystallization temperature (T_c) plot (Fig. 9) equilibrium melting temperature (T_m^{eq}) were obtained. These data can be well fitted by Hoffman-weeks equation[37].

$$T_m^{'} = \emptyset T_c + (1 - \emptyset) T_m^{eq} \quad (6)$$

where $\emptyset = \frac{1}{\gamma}$ is the stability parameter and γ is the ratio of the lamellar thickness to the initial lamella thickness l^*at T_c. In this equation, $\emptyset$ varies from 0 to 1. $\emptyset = 0$ suggests $T_m^{'} = T_m^{eq}$, whereas $\emptyset = 1$

suggests $T_m^{'} = T_c$. Thus, at $\emptyset = 1$crystals are intrinsically unstable while the most stable crystals is at $\emptyset = 0$. It is clear from Fig. 9 that equilibrium melting temperatures for dynamically vulcanized and unvulcanized samples depressed by increasing the amorphous component content, furthermore T_m^{eq} values of vulcanized samples are higher. Besides, $\emptyset$ values of dynamically vulcanized blends are around 0.35 while this parameter is around 0.25 for unvulcanized blends; therefore, the stability of the crystals in the dynamically vulcanized samples is lower than unvulcanized one.

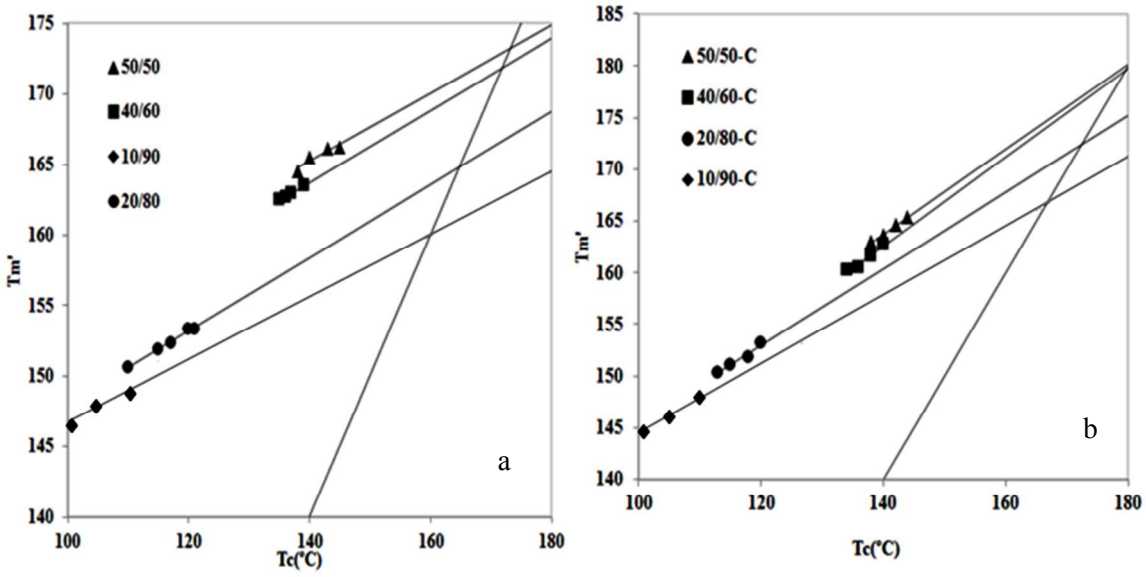

Figure9. H-W plot for a) miscible blends, b) dynamically vulcanized samples

Temperature dependence of K_n

Hoffman secondary nucleation theory is a common method for evaluating kinetics of crystallization in miscible blends [38-44]. For analyzing the growth of spherulites in a miscible blends:

$$G = G_0 \exp\left(\frac{-\Delta G_\eta}{RT_c}\right) \exp\left(\frac{\Delta G^*}{KT_c}\right) \quad (7)$$

where ΔG_η is the activation energy required for crystallizing segment to diffuse through the phase boundary, ΔG^* the free energy of crystallization of the initial lamella, $\emptyset_2$ is the PVDF volume fraction, K

Boltzmann constant (1.38×10^{-16} erg.K^{-1}), G_0 a constant, R the universal constant for gases and T_c temperature of crystallization in K.

$\Delta G_\eta / RT_c$ can be describe as:

$$\frac{\Delta G_\eta}{RT_c} = \frac{C_1}{R(C_2 + T_c - T_g)} \quad (8)$$

where C_1 is 4120 cal mol^{-1}, C_2 is 51.6K and T_g is glass transition temperature in K. Combining Boon [3] theory with a crystallization regime concepts [45], ΔG^* is describing as:

$$\frac{\Delta G^*}{K_B T_c} = \frac{K_g}{f T_c \Delta T} - \frac{2\sigma T_m^{eq}}{b_0 \Delta H_f \Delta T} \ln \phi_2 \quad (9)$$

$$K_g = \frac{Z b_0 \sigma \sigma_e T_m^{eq}}{K_B \Delta H_f} \quad (10)$$

$$f = \frac{2T_c}{T_m^{eq} + T_c} \quad (11)$$

where $\Delta H_f (= 1.986 \times 10^9 \text{ erg Cm}^{-3})$ is the heat of fusion per unit volume of PVDF, f is the modification factor of heat of fusion, k_g is the nucleation factor, σ the free energy of side surface of nucleus, σ_e the free energy of fold surface of nucleus, $\Delta T = T_m - T_c$, b_0 (=4.45 A^0) the thickness of a monomolecular layer of PVDF [46], z is a constant associated to the regime of crystallization (Z=4 for regimes I and III; Z=2 for regime II) for the rate of overall crystallization, one can assume $G = CK_n^{1/n}$, where C is a constant. Assuming that $\sigma = 0.1\ (\Delta H_f)(a_0 b_0)^{1/2}$ where a_0 is the monomolecular width of PVDF (5.43 Å) and combining relations (7), (8) and (9) the following equation is attained:

$$f(K_n) = \frac{1}{n} \ln K_n - \ln \phi_2 + \frac{C_1}{R(C_2 + T_c - T_g)} - \frac{0.2\, T_m^{eq} \ln \phi_2}{\Delta T} = \ln A_0 - \frac{K_g}{f T_c \Delta T} \quad (12)$$

The plots of f(K_n) vs. 1/ $fT_c\Delta T$ for the simple miscible and dynamically vulcanized blends are shown in Fig.10. Fitting the experimental data results a straight lines. A_0 and K_g attained from intercepts and slopes of these lines and listed in Table 3.

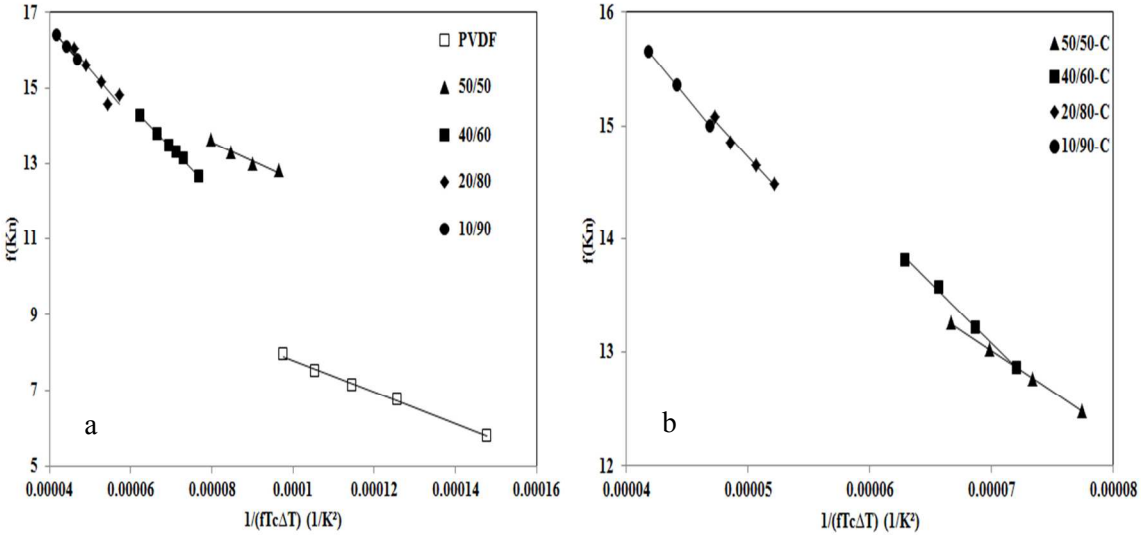

Figure10. f(K_n) vs. 1/ f$T_c\Delta T$ for a) neat PVDF, unvulcanized blends and b)dynamically vulcanized blends.

Table 3. Values of Kg, $\sigma\sigma_e$, $\sigma_e$and A_0 from data analysis.

PVDF-ACM	Kg(K^2)	$\sigma\sigma_e$(erg^2/cm^4)	σ_e(erg/cm^2)	A_0
PVDF	40755	271	27	11.99
50/50	100258	666	68	17.53
40/60	110440	734	75	21.16
20/80	126951	844	86	20.82
10/90	132666	882	90	21.81
50/50-C	72151	479	49	18.06
40/60-C	105439	701	71	20.46
20/80-C	117282	779	79	20.58
10/90-C	131465	874	89	21.06

The Lauritzen Z test is commonly used for distinguish of crystallization regime I or II.

$$z \approx 10^3 (^{l}/_{2a_0})^2 \exp(-x/(T_c\,\Delta T)) \quad (13)$$

$$x = kg\ for\ test\ of\ regime\ I, z \leq 0.01$$

$$x = 2kg\ for\ test\ of\ regime\ II, z \geq 0.1$$

where l is the thickness of lamella. Lauritzen z test calculation indicates that crystallization take place at regime II. However, there was no specific regime transition in plot of f(K_n) vs. $1/fT_c\Delta T$ for all the samples as shown in Fig.10.

The value of $\sigma\sigma_e$ (Table3) for each sample was obtained by applying K_g and z=2 to equation 10. Assuming that the value of σ for neat PVDF and sample is equal and using the value of σ to be 9.76 erg.cm^{-2} as reported in the literature [46], σ_e might be evaluated as described in Table3. It is clear from Table3 that the values of σ_e for PVDF/ACM miscible blend increased by increment of noncrystallizable phase percent in the blend. It is known that amorphous molecule can readily fold around PVDF chains, results the development of bulky loop on the PVDF lamellar surface[8]. This phenomenon will result the rise on the surface entropy and enthalpy of folding (σ_e=He-TSe) [47]. However, σ_e values of dynamically vulcanized samples are lower than unvulcanized one especially for 50/50-C sample. Decrease in σ_e values of 50/50 blend upon dynamic vulcanization can be related to rejection of ACM chains from PVDF's lamellas because 50/50 sample composition is near the binodal curve[2] therefore its motivation for phase separation is strong. However, it seems that increasing the molecular weight as a result of crosslinking facilitated the phase decomposition of the 50/50 blend; because this sample is not far into miscible region. Therefore, again fold surface free energy measurement confirms our previous morphological observation[4] and correlate well to SEM and SAXS results. However, it seems that free energy of folding values can act as a tool to predict the state of phase separation upon dynamic vulcanization in this system.

Conclusion

The main goal of this study is to investigate how dynamic vulcanization of a miscible crystalline/amorphous blend affects the crystallization kinetics of crystallizable component. The observed morphology was interesting; dynamic vulcanization of 50/50 blend which is near the binodal curve resulted the nano-phase decomposed structure whereas other miscible blends which their composition is deep into miscible region didn't display any sign of dynamic vulcanization induce phase decomposition. Small Angel X-ray Scattering results showed that the amorphous layer thickness, and long period decreased with dynamic vulcanization and this decrease is more pronounced for 50/50 blend compare to other samples. Fourier Transform Infra-Red analysis demonstrated that blending and dynamic vulcanization does not induce creation of polymorphic crystalline forms of PVDF. Overall crystallization rate results were evaluated using real-time Fourier Transform Infra-Red and Differential Scanning Calorimetery techniques. It was demonstrated that dynamic vulcanization decreased the overall crystallization rate of PVDF compared to unvulcanized blends. Furthermore, it was shown that Avrami parameter (n) values for dynamically vulcanized samples are higher than that of equivalent unvulcanized blends. This can be related to the mechanism of branching of polymer crystals imposed to the system upon topological constraint of 3D network of crosslinked samples. Using Lauritzen-Hoffman model we showed that free energy of folding decreased for dynamically vulcanized sample compare to unvulcanized blends, which means that ACM chains were rejected from the gallery of lamellas upon dynamic vulcanization, therefore our isothermal crystallization study confirmed our morphological observations. Furthermore we demonstrated that free energy of folding values can act as a tool to predict the state of phase separation upon dynamic vulcanization.

References

[1] R. Holyst, Soft Matter, 1 (2005) 329-333.
[2] M. Abolhasani, A. Jalali-Arani, H. Nazockdast, Q. Guo, Polymer, 54 (2013) 4686-4701.
[3] J. Boon, J.M. Azcue, Journal of Polymer Science Part A-2: Polymer Physics, 6 (1968) 885-894.
[4] M.L. Di Lorenzo, P. Rubino, M. Cocca, European polymer journal, 49 (2013) 3309-3317.
[5] M. Weng, Z. Qiu, Industrial & Engineering Chemistry Research, 52 (2013) 10198-10205.
[6] Z. He, Y. Liang, P. Wang, C.C. Han, Polymer, 54 (2013) 2355-2363.

[7] M. Pracella, Handbook of Polymer Crystallization, (2013) 287-326.
[8] Q. Guo, G. Groeninckx, Polymer, 42 (2001) 8647-8655.
[9] Y. Li, Y. Oono, Y. Kadowaki, T. Inoue, K. Nakayama, H. Shimizu, Macromolecules, 39 (2006) 4195-4201.
[10] Q. Guo, C. Harrats, G. Groeninckx, M. Koch, Polymer, 42 (2001) 4127-4140.
[11] Q. Guo, C. Harrats, G. Groeninckx, H. Reynaers, M. Koch, Polymer, 42 (2001) 6031-6041.
[12] S. Zheng, H. Zheng, Q. Guo, Journal of Polymer Science Part B: Polymer Physics, 41 (2003) 1085-1098.
[13] Q. Guo, R. Thomann, W. Gronski, T. Thurn-Albrecht, Macromolecules, 35 (2002) 3133-3144.
[14] R.M.A. l'Abee, J.G.P. Goossens, M. van Duin, Rubber chemistry and technology, 80 (2007) 311-323.
[15] A. Ramanujam, K. Kim, T. Kyu, Polymer, 41 (2000) 5375-5383.
[16] P. Martins, A. Lopes, S. Lanceros-Mendez, Progress in polymer science, 39 (2014) 683-706.
[17] A.C. Lopes, C. Caparros, S. Ferdov, S. Lanceros-Mendez, Journal of Materials Science, 48 (2013) 2199-2206.
[18] P. Martins, C.M. Costa, J. Ferreira, S. Lanceros-Mendez, The Journal of Physical Chemistry B, 116 (2012) 794-801.
[19] M.M. Abolhasani, Q. Guo, A. Jalali-Arani, H. Nazockdast, Journal of Applied Polymer Science, 130 (2013) 1247-1258.
[20] M.M. Abolhasani, F. Zarejousheghani, M. Naebe, Q. Guo, Soft Matter, (2014).
[21] O. Glatter, O. Kratky, Small angle X-ray scattering, Academic press London, 1982.
[22] G. Strobl, M. Schneider, I. Voigt-Martin, Journal of Polymer Science: Polymer Physics Edition, 18 (1980) 1361-1381.
[23] Q. Guo, P. Figueiredo, R. Thomann, W. Gronski, Polymer, 42 (2001) 10101-10110.
[24] M.M. Abolhasani, M. Naebe, A. Jalali-Arani, Q. Guo, PloS one, 9 (2014) e88715.
[25] M. Sharma, G. Madras, S. Bose, Physical Chemistry Chemical Physics, (2014).
[26] M.M. Abolhasani, M. Naebe, Q. Guo, Physical Chemistry Chemical Physics, 16 (2014) 10679-10687.
[27] M. Silva, V. Sencadas, G. Botelho, A. Machado, A.G. Rolo, J. Rocha, S. Lanceros-Mendez, Materials Chemistry and Physics, 122 (2010) 87-92.
[28] P. Martins, C.M. Costa, S. Lanceros-Mendez, Applied Physics A, 103 (2011) 233-237.
[29] J. Gomes, J.S. Nunes, V. Sencadas, S. Lanceros-Mendez, Smart Materials and Structures, 19 (2010) 065010.
[30] M. Silva, V. Sencadas, A. Rolo, G. Botelho, A.V. Machado, J.G. Rocha, S. Lanceros-Méndez, in: Materials Science Forum, Trans Tech Publ, 2008, pp. 534-537.
[31] K. Asai, M. Okamoto, K. Tashiro, Polymer, 49 (2008) 5186-5190.
[32] A. Melvin, The Journal of Chemical Physics, 7 (1939) 1103-1112.
[33] Z. Qiu, C. Yan, J. Lu, W. Yang, Macromolecules, 40 (2007) 5047-5053.
[34] B. Wunderlich, Macromolecular physics, Elsevier, 2012.
[35] D. Grenier, P. Homme, Journal of Polymer Science: Polymer Physics Edition, 18 (1980) 1655-1657.
[36] L. Morgan, Philosophical Transactions of the Royal Society of London. Series A, Mathematical and Physical Sciences, 247 (1954) 13-22.
[37] J.D. Hoffman, J.J. Weeks, J Res Natl Bur Stand A, 66 (1962) 13-28.
[38] J. Hoffman, G.T. Davis, J. Lauritzen, N. Hannay, Hannay, NB, Ed, (1976) 497.
[39] J. Hoffman, CAS, Web of Science® Times Cited, 386.
[40] J.D. Hoffman, C.M. Guttman, E.A. DiMarzio, Faraday Discussions of the Chemical Society, 68 (1979) 177-197.
[41] J.D. Hoffman, J. Lauritzen, Journal of Research of the National Bureau of Standards, (1961) 297-+.
[42] J.D. Hoffman, R.L. Miller, Polymer, 38 (1997) 3151-3212.
[43] J.I. Lauritzen Jr, J.D. Hoffman, Journal of applied Physics, 44 (2003) 4340-4352.

[44] J. Lauritzen, J.D. Hoffman, J. Res. Natl. Bur. Stand. A, 64 (1960) 73-102.
[45] T. Wang, T. Nishi, Macromolecules, 10 (1977) 421-425.
[46] J.S. Lee, K.J. Kim, Fibers and Polymers, 8 (2007) 237-242.
[47] E. Martuscelli, M. Pracella, P.Y. Wang, Polymer, 25 (1984) 1097-1106.

Is it possible to find the state of phase separation using investigation of free energy of folding parameter?